measured by cyclic voltammetry, is the largest for all of the complexes listed in Table IV. Thus, from the spectral changes observed in the oxidation of an alcohol by $[(bpy)_2(PMe_3)Ru^{IV}(O)]^{2+}$ (Figure 12), the kinetics of substrate oxidation are complicated, because a Ru^{III}–OH intermediate is observed and can function as a one-electron oxidant, independent of the Ru^{IV}=O oxidation chemistry.

Conclusion

The synthetic chemistry of ruthenium(II) complexes which utilize bipyridine and pnictogen ligands has been developed in the systematic preparation of a variety of $[(bpy)_2(PnR_3)Ru^{II}(OH_2)](ClO_4)_2$ complexes, which can be oxidized under mild conditions to the analogous ruthenium(IV)–oxo complexes. These syntheses demonstrate that, under appropriate conditions, easily oxidized pinctogen ligands remain *intact* in the coordination sphere of a potent oxidizing metal center, such as ruthenium(IV)–oxo, to generate fundamentally new ruthenium complexes. Thus, pinctogen ligands can now be used to control the redox potentials of the available ruthenium-centered redox couples, to solubilize the ruthenium(IV)–oxo complexes in both polar and less polar solvents, to kinetically limit the formation of ruthenium(III) from ruthenium(II) and ruthenium(IV), and to exert unusual ligand properties, such as hydrophobic effects or catalytic properties, on the substrate oxidation chemistry of the ruthenium(IV)–oxo moiety.

Acknowledgment. This work was supported in part by the donors of the Petroleum Research Fund, administered by the American Chemical Society, the Cottrell Research Corportion, and both the Biomedical Research Support Grant and the Research Development Fund of SUNY at Buffalo. In addition, the authors gratefully acknowledge the contributions of Stephen A. Kubow to this paper.

Registry No. *cis*-$Ru^{II}(bpy)_2Cl_2$, 19542-80-4; *cis*-$[(bpy)_2PMe_3Ru^{II}Cl](ClO_4)$, 112088-07-0; *cis*-$[(bpy)_2PEt_3Ru^{II}Cl](ClO_4)$, 99687-22-6; *cis*-$[(bpy)_2P(n\text{-}Pr)_3Ru^{II}Cl](ClO_4)$, 112088-09-2; *cis*-$[(bpy)_2P(i\text{-}Pr)_3Ru^{II}Cl](ClO_4)$, 112088-11-6; *cis*-$[(bpy)_2P(n\text{-}Bu)_3Ru^{II}Cl](ClO_4)$, 112088-12-7; *cis*-$[(bpy)_2PCy_3Ru^{II}Cl](ClO_4)$, 112088-14-9; *cis*-$[(bpy)_2PBz_3Ru^{II}Cl](ClO_4)$, 112088-16-1; *cis*-$[(bpy)_2PPh_3Ru^{II}Cl](ClO_4)$, 112088-17-2; *cis*-$[(bpy)_2AsPh_3Ru^{II}Cl](ClO_4)$, 103727-05-5; *cis*-$[(bpy)_2SbPh_3Ru^{II}Cl](ClO_4)$, 112088-18-3; *cis*-$[(bpy)_2P(p\text{-}CF_3C_6H_4)_3Ru^{II}Cl](ClO_4)$, 112088-20-7; *cis*-$[(bpy)_2PMe_3Ru^{II}OH_2](ClO_4)_2$, 112088-22-9; *cis*-$[(bpy)_2PEt_3Ru^{II}OH_2](ClO_4)_2$, 99705-87-0; *cis*-$[(bpy)_2P(n\text{-}Pr)_3Ru^{II}OH_2](ClO_4)_2$, 112112-48-8; *cis*-$[(bpy)_2P(i\text{-}Pr)_3Ru^{II}OH_2](ClO_4)_2$, 112088-24-1; *cis*-$[(bpy)_2P(n\text{-}Bu)_3Ru^{II}OH_2](ClO_4)_2$, 112088-26-3; *cis*-$[(bpy)_2PCy_3Ru^{II}OH_2](ClO_4)_2$, 112088-28-5; *cis*-$[(bpy)_2PBz_3Ru^{II}OH_2](ClO_4)_2$, 112088-30-9; *cis*-$[(bpy)_2PPh_3Ru^{II}OH_2](ClO_4)_2$, 111743-41-0; *cis*-$[(bpy)_2AsPh_3Ru^{II}OH_2](ClO_4)_2$, 112088-32-1; *cis*-$[(bpy)_2SbPh_3Ru^{II}OH_2](ClO_4)_2$, 112088-34-3; *cis*-$[(bpy)_2P(p\text{-}CF_3C_6H_4)_3Ru^{II}OH_2](ClO_4)_2$, 112088-36-5; *cis*-$[(bpy)_2SbPh_3Ru^{II}NO_2](ClO_4)$, 112088-38-7; *cis*-$[Ru(bpy)_2(NO)(NO_2)](ClO_4)_2$, 112088-39-8; *cis*-$[(bpy)_2SbPh_3Ru^{II}(NO)](ClO_4)_3$, 112088-41-2; *cis*-$[(bpy)_2(PMe_3)Ru^{IV}(O)](ClO_4)_2$, 112088-43-4; *cis*-$[(bpy)_2(PEt_3)Ru^{IV}(O)](ClO_4)_2$, 99687-21-5; *cis*-$[(bpy)_2(P\text{-}i\text{-}Pr_3)Ru^{IV}(O)](ClO_4)_2$, 112088-45-6; *cis*-$[(bpy)_2(PPh_3)Ru^{IV}(O)](ClO_4)_2$, 111743-44-3; *cis*-$[(bpy)_2(AsPh_3)Ru^{IV}(O)](ClO_4)_2$, 112088-47-8; *cis*-$[(bpy)_2(PCy_3)Ru^{IV}(O)](ClO_4)_2$, 112088-49-0; *cis*-$[(bpy)_2(PBz_3)Ru^{IV}(O)](ClO_4)_2$, 112088-51-4; *cis*-$[(bpy)_2(PEt_3)Ru^{III}OH](ClO_4)_2$, 112088-52-5; *cis*-$[(bpy)_2(PEt_3)Ru^{IV}(^{18}O)](ClO_4)_2$, 112088-54-7; $RuCl_3$, 10049-08-8.

Supplementary Material Available: Elemental analyses of complexes (Table I) (2 pages). Ordering information is given on any current masthead page.

Molecular Design Based on Inclusion Chemistry. Synthesis, Characterization, and Crystal Structures of a New Family of Lacunar Schiff Base Complexes with Promise as Broad-Range Host Molecules

Dorai Ramprasad, Wang-Kan Lin, Kenneth A. Goldsby, and Daryle H. Busch*

Contribution from the Chemistry Department, The Ohio State University, 120 West 18th Avenue, Columbus, Ohio 43210. *Received March 30, 1987*

Abstract: An entirely new family of lacunar Schiff base nickel(II) complexes is reported. The new species provide a protected void or lacuna in the vicinity of a coordination site at the metal ion, which may facilitate reversible O_2 binding by derivatives of appropriate metal ions. The lacunar ligands are prepared by adding a long bridging group that spans the plane of the well-known Schiff base ligand bis(acetylacetone)ethylenediamine. The bridging linkage, which serves as the roof of the lacuna, contains aromatic groups as risers linked to polymethylene chain through heteroatoms that provide flexible points within the bridge structure. Ease of synthesis has been a consideration in ligand design. Two crystal structures have been determined on nickel(II) derivatives of ligands of this class. The results show that the orientation of the roof of the lacuna relative to the approximately planar parent Schiff base ligand is dependent on the substituents on the β-diketone moiety. $[Ni(Me_2R^2Me_2malen)]\cdot 2CHCl_3$ crystallizes in the monoclinic space group $P2_1/c$ with $a = 10.608$ (2) Å, $b = 18.388$ (4) Å, $c = 20.492$ (4) Å, $\beta = 95.35$ (2)°, and $Z = 4$. The structure refined to $R = 0.051$ and $R_w = 0.050$ for 4078 reflections with $F_o^2 > 3\sigma(F_o^2)$. The bridge projects above the coordination plane giving a substantial cavity. Solvent molecules flank the cavity. $[Ni(Me_2R^2H_2malen)]\cdot CH_2Cl_2$ is in monoclinic space group $P2_1/n$ with $a = 13.205$ (3) Å, $b = 17.497$ (3) Å, $c = 14.315$ (5) Å, $\beta = 93.59$ (2)°, and $Z = 4$. $R = 0.106$ and $R_w = 0.092$ for 3496 reflections with $F_o^2 > 3\sigma(F_o^2)$. The bridge is not held vertically above the coordination plane. The difference in structures is attributed to the presence or absence of pairs of methyl groups on the β-diketone moieties.

The evolution of the broad chemistry of macrocyclic ligands constitutes one of the major pillars[1] of the enormous research subject bearing the title "inclusion chemistry".[2] Metal coordination by such entities constituted the principal activity during the founding years for that part of the field that derived from early

(1) See: Izatt, R. M., Christensen, J. J., Eds. *Advances in Macrocycle Chemistry*; Wiley: New York, 1987; Vol. 3, and reviews and references therein.

(2) Broadly defined, inclusion chemistry incorporates all those chemical species, whether they be continuous solids or discrete molecules, having voids or cavities of molecular dimension, and all of the related chemical association and other reaction chemistry. Implicit in the name is the capability of *including* some other molecular entities within the cavities.

0002-7863/88/1510-1480$01.50/0

studies on macrocyclic complexes of transition-metal ions.[3-8] Host/guest chemistry extended the original domain to all manner of small molecule or ion inclusion within the "void" or cavity that is implicitly a part of the structure of the host molecule.[9-17] The union of host/guest chemistry with macrocyclic ligand chemistry has added dimensions to the subject of inclusion chemistry. Molecules with separate chambers designed to accommodate diverse occupants, e.g., metal ions, organic guest molecules, and small coordinated ligands, are serving to control a multiplicity of structural variables, each of which may regulate only a single aspect of the total function of the intricately designed molecular entity. The new compounds presented here have been designed in this context.

Previously studied systems having the capability of enclosing a metal ion within a polyfunctional chelating ligand and simultaneously encompassing additional species were most frequently based on porphyrin ligands. We have designed and characterized a very broad family of non-porphyrin "cyclidiene" ligand derivatives (structures I–III) that have produced several classes of

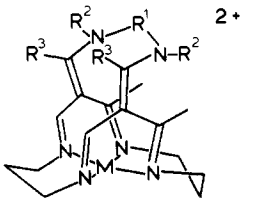

I

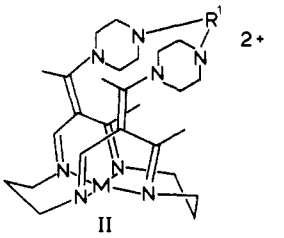

II

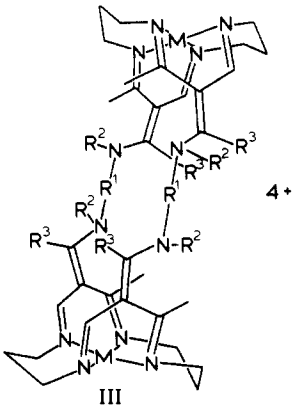

III

highly specialized and distinctly facilitated, functional molecular entities. These include new iron and cobalt oxygen carriers (structure I),[18-22] transition-metal host species that regiospecifically bind aliphatic or aromatic molecules through hydrophobic interactions (structure II),[23-27] and mono- and dinucleating (structure III) species capable of simultaneously binding dioxygen, or some other small ligand, and an organic guest molecule.[28,29] The study of those species has yielded relationships that can only be tested for generality by producing and studying new families of compounds with parallel capabilities. We report here the second family of completely synthetic lacunar complexes that gives promise of a similarly rich inclusion chemistry.

The new ligands are derived from one of the most common and longest known categories of cobalt/oxygen carriers—the complexes of Schiff base ligands.[30] These ligands characteristically have two oxygen and two nitrogen donors and bear a charge of 2–. They are most often formed by the Schiff base condensation of 2 mol of an aromatic *o*-hdyroxy carboxaldehyde or a β-diketone with a diamine. The broadest families of these species are those related to salen (structure IV)[31,32] and acacen (structure V).[33,34] An

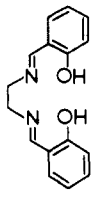

IV

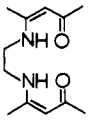

V

innovative attempt to produce a lacunar oxygen carrier of the Schiff base type was reported by Martin et al. by use of a diamine that rose above the coordination plane leaving a protected cavity.[35,36] Unfortunately, the cavities of that family of species were too small to permit effective oxygen binding.

We describe our new ligands as lacunar *malen* derivatives. They are of general structure VI in which the parent Schiff base is

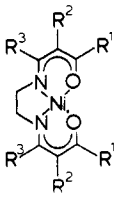

VI

theoretically derived from malonaldehyde and a simple diamine such as ethylenediamine. Readily accessible examples involve alkyl or aryl substituents at all or part of the R^1 and R^3 positions. The lacuna is produced by bridging between the central carbon atoms of the two malonaldehyde moieites with specially designed "straps"

(3) Izatt, R. M. Christensen, J. J., Eds. *Advances in Macrocycle Chemistry*; Wiley: New York, 1979, 1981; Vol. 1–2.
(4) Melson, G. A., Ed. *Coordination Chemistry of Macrocyclic Compounds*; Plenum: New York, 1979.
(5) Busch, D. H. *Acc. Chem. Res.* **1978**, *11*, 392.
(6) Lindoy, L. F.; Busch, D. H. *Preparative Inorganic Reactions*; Jolly, W. L., Ed.; Interscience: New York, 1971; Vol. 6.
(7) Busch, D. H. *Helv. Chim. Acta* **1967**, pp 174–206 (Werner Commemoration Volume).
(8) Busch, D. H. *Rec. Chem. Prog.* **1964**, *25*, 107.
(9) Cram, D. J.; Cram, J. M. *Science (Washington, D.C.)* **1974**, *183*, 803.
(10) Cram, D. J. *Science (Washington, D.C.)* **1983**, *219*, 1177.
(11) Saenger, W. *Angew. Chem., Int. Ed. Engl.* **1980**, *19*, 344.
(12) Tabushi, I. *Accts. Chem. Res.* **1982**, *15*, 66.
(13) Breslow, R. *Chem. Br.* **1983**, 128.
(14) Breslow, R. *Adv. Chem. Ser.* **1980**, No. *191*, 1.
(15) Lehn, J.-M. *Struct. Funct. Enzyme Catal.* **1981**, 24.
(16) Lehn, J.-M. *Acc. Chem. Res.* **1978**, *11*, 49.
(17) Meade, T. J.; Busch, D. H. *Prog. Inorg. Chem.* **1985**, *33*, 59.
(18) Stevens, J. C.; Busch, D. H. *J. Am. Chem. Soc.* **1980**, *102*, 3285.
(19) Herron, N.; Busch, D. H. *J. Am. Chem. Soc.* **1981**, *103*, 1236.
(20) Herron, N.; Cameron, J. H.; Neer, G. L.; Busch, D. H. *J. Am. Chem. Soc.* **1983**, *105*, 298.
(21) Herron, N.; Zimmer, L. L.; Grzybowski, J. J.; Olszanski, D. J.; Jackels, S. C.; Callahan, R. W.; Cameron, J. H.; Christoph, G. G.; Busch, D. H. *J. Am. Chem. Soc.* **1983**, *105*, 6585.
(22) Busch, D. H. *Crit. Care Med.* **1982**, *10*(4), 246.
(23) Takeuchi, K. J.; Busch, D. H. *J. Am. Chem. Soc.* **1981**, *103*, 2421.
(24) Kwik, W.-L.; Herron, N.; Takeuchi, K. J.; Busch, D. H. *J. Chem. Soc., Chem. Commun.* **1983**, 409.
(25) Takeuchi, K. J.; Alcock, N. W.; Busch, D. H. *J. Am. Chem. Soc.* **1983**, *105*, 4261.
(26) Takeuchi, K. J.; Busch, D. H. *J. Am. Chem. Soc.* **1983**, *105*, 6812.
(27) Meade, T. J.; Kwik, W.-L.; Herron, N.; Alcock, N. W.; Busch, D. H. *J. Am Chem. Soc.* **1986**, *108*, 1954.
(28) Meade, T. J.; Takeuchi, K. J.; Busch, D. H. *J. Am. Chem. Soc.* **1987**, *109*, 725.
(29) Meade, T. J.; Hoshino, N.; Ye, N.; Busch, D. H., unpublished results.
(30) Tsumaki first recognized O_2 binding by a Schiff base complex in 1938. See, for example: Jones, R. D.; Summerville, D. A.; Basolo, F. *Chem. Rev.* **1979**, *79*, 139.
(31) Floriani, C.; Calderazzo, F. *J. Chem. Soc. A* **1969**, 946.
(32) Calderazzo, E.; Floriani, C.; Salzmann, J. J. *Inorg. Nucl. Chem. Lett.* **1966**, *2*, 379.
(33) Crumbliss, A. L.; Basolo, F. *Science (Washington, D.C.)* **1969**, *164*, 1168.
(34) Crumbliss, A. L.; Basolo, F. *J. Am. Chem. Soc.* **1970**, *92*, 55.
(35) Martin, R. L.; Henrickson, A. R.; Hope, J. M. *J. Chem. Soc., Dalton Trans.* **1979**, 1497.
(36) Martin, R. L.; Baker, A. T.; Taylor, D. *J. Chem. Soc., Dalton Trans.* **1979**, 1503.

(structure VII). The terminal acyl groups place electron-with-

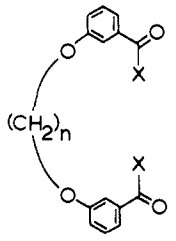

VII

drawing substituents on the parent ligand, and this has been shown to enhance both the longevity and the dioxygen affinity of the corresponding cobalt oxygen carriers.[37] The acyl groups are aromatic, and because of their rigid structures they serve as risers, lifting the bridging group above the coordination plane. The actual bridges are polymethylene linkages that attach to the aromatic risers through ether oxygens. Those heteroatoms provide a hingelike flexibility and help shape the cavity. The use of aromatic acyl groups also obviates a difficulty associated with aliphatic acylating agents, their tendency to eliminate HX and form ketenes.[38] We report here the design, synthesis, and characterization of these extremely promising new compounds, including two X-ray structure determinations.

Results and Discussion

Synthesis and Characterization. The first synthetic target in these studies was VIII with $R^1 = CH_3$ and $R^3 = H$. Attention

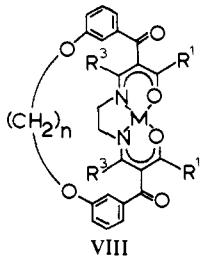

VIII

was focused on this complex because of the very promising properties reported for the corresponding nonlacunar Schiff base complex of cobalt(II).[37] The synthesis proceeded on the basis of the well-known reactivity of the parent complexes (structure VI) with electrophiles.[39,40]

Model reactions were used to characterize the synthetic process before turning to the more demanding ring closure. The precursor complex (VI, M = Ni, $R^1 = CH_3$, $R^2 = R^3 = H$) and 2 equiv of both acetyl chloride and triethylamine were held at reflux in acetonitrile solution for 3 days. This yielded the monoacylated derivative. In contrast, the same reaction with 2 equiv of benzoyl chloride produced the desired diacylation. These results indicated that the nickel complex of this particular ligand is a weak nucleophile since only the more powerful electrophile drove the reaction to completion.

The choice of diacyl halide for the ring-closure reaction is critical. Because of the limited nucleophilic character of the reactant complex, bridging reagents subject to competing side reactions are likely to be ineffective. This is true of aliphatic diacyl halides since they form ketenes and ketene dimers in the presence of bases such as triethylamine.[38] Thus, both their enhanced electrophilicity and the absence of deleterious side reactions favored aromatic acyl groups for this process.

Because the parent Schiff base ligand is approximately planar, the formation of a substantial cavity requires a strap that lifts

Scheme I

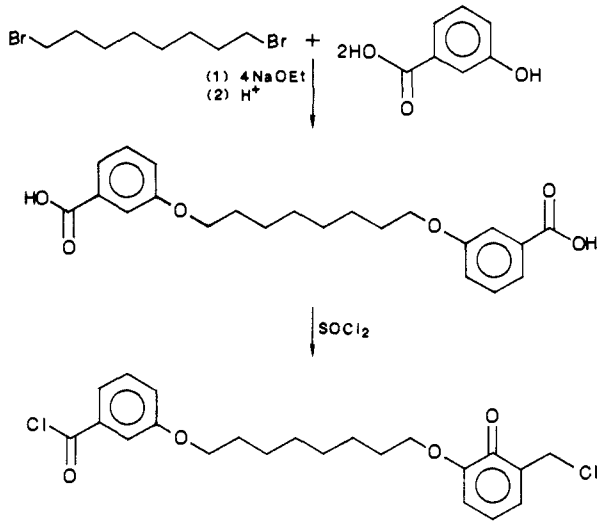

the bridge above the coordination plane. Studies with capped porphyrins have shown the undesirable consequences of relatively collapsible superstructures.[41,42] The strap having structure VII was chosen for these reasons along with other structural considerations. The ether linkages greatly facilitated the synthesis of the strap.

As shown in Scheme I, the synthesis of the bridging reagent VII proceeds by the deprotonation of 2 equiv of *m*-hydroxybenzoic acid and its subsequent reaction with 1 mol of 1,8-dibromooctane. Since the phenoxide ion is a better nucleophile than the carboxylate ion, the desired ether linkages form. Refluxing this product with thionyl chloride yields the necessary diacyl halide. The infrared spectrum of the diacyl chloride gave strong bands at 1770 and 1750 cm^{-1} that are attributable to the carbonyl stretching vibration. The splitting may derive from Fermi resonance. The ^{13}C NMR spectrum shows 11 distinct peaks, the values of which are listed in Table I.

At this stage, a further model reaction was used to demonstrate that the addition of the ether group to the electrophile does not jeopardize its reactivity. *m*-Anisoyl chloride was added to the nickel complex (structure VI) to give [Ni(R^1_2(Anyl)$_2R^3_2$malen)] (anisoyl is abbreviated Anyl) (IX). The meta substituent was

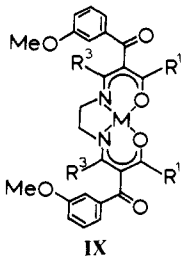

IX

chosen partially to minimize the electron density at the acyl carbon; this isomer was also most desirable from the stereochemical standpoint. The diacylated product was formed in good yield after reflux, for 2–3 days, of a solution containing VI ($R^1 = R^3 = CH_3$ or $R^3 = CH_3$, $R^1 = H$) and 2 equiv of both *m*-anisoyl chloride and triethylamine in dry benzene. This was most encouraging since reaction at both sites on the parent complex is an absolute requirement for the related ring-closure process.

The unbridged derivatives (structure IX) that were prepared in model reactions were characterized by their infrared spectra (Table II), ^{13}C NMR spectra (Table I), and elemental analyses (Table III). The presence of the C=O stretching band in the region around 1650 cm^{-1} in their infrared spectra provided the first identification while the mirror symmetry required for di-

(37) Kubokura, K.; Okawa, H.; Kida, S. *Bull. Chem. Soc. Jpn.* **1978**, *51*, 2036.
(38) Hanford, W. E.; Sauer, J. C. *Organic Reactions*; Wiley: New York, 1946; Vol. III, p 129.
(39) Kenney, J. W.; Nelson, J. H.; Henry, R. A. *J. Chem. Soc., Chem. Commun.* **1973**, 690.
(40) Howells, P. N.; Kenney, J. W.; Nelson, J. H.; Henry, R. A. *Inorg. Chem.* **1976**, *15*, 124.
(41) Hashimoto, T.; Dyer, R. L.; Crossley, M. J.; Baldwin, J. E.; Basolo, F. *J. Am. Chem. Soc.* **1982**, *104*, 2101.
(42) Sabat, M.; Ibers, J. A. *J. Am. Chem. Soc.* **1982**, *104*, 3715.

Table I. $^{13}C\{^1H\}$ NMR Data for Complexes and Ligands in $CDCl_3$ Solution (Relative to Me_4Si)

compound	R^1	R^3	shifts, ppm
VIII (lacunar)	CH_3	CH_3	198.4, 177.1, 164.0, 159.3, 141.6, 130.0, 120.3, 118.5, 117.3, 113.6, 68.6, 53.2, 29.7, 29.5, 25.8, 24.9
VIII (lacunar)	CH_3	H	194.6, 187.5, 160.6, 158.3, 142.3, 130.2, 120.9, 118.1, 115.6, 113.2, 68.3, 57.9, 29.7, 29.4, 26.3, 25.8
IX	CH_3	CH_3	198.3, 177.5, 164.6, 160.0, 141.6, 129.6, 122.4, 119.5, 113.8, 113.4, 55.5, 53.4, 25.1, 20.3
IX	CH_3	H	194.7, 187.8, 160.6, 159.6, 142.6, 129.2, 121.1, 117.3, 113.4, 58.2, 55.3, 26.9
VIII			168.2, 159.4, 134.4, 129.8, 123.9, 122.3, 116.1, 68.4, 29.2, 29.1, 25.9

Table II. Selected Infrared Bands for the New Complexes

complex	R^1	R^3	CO, cm^{-1}	ν_{CN}, ν_{CC}, cm^{-1}
VIII	CH_3	CH_3	1650	1555
VIII	CH_3	H	1640	1590
IX	CH_3	CH_3	1650	1555
IX	CH_3	H	1635	1590

substitution was readily evident in their ^{13}C NMR spectra.

The ring closure also presents the possibility of forming dimers and higher oligomers. Therefore, all bridging reactions were conducted at high dilution. The lacunar complexes were formed by refluxing VI ($R^1 = R^3 = CH_3$ or $R^1 = CH_3$, $R^3 = H$) with VII and an excess of triethylamine in a large reservoir of benzene for as long as 1 week. After filtration of the triethylamine hydrochloride, the solvent was removed, and the resulting product was chromatographed on an alumina column. An orange-red band was eluted with chloroform, and the lacunar complex VIII was obtained by crystallization from mixtures of chloroform and hexane.

The new lacunar complexes were characterized by elemental analyses (Table III), mass spectra, infrared spectra (Table II), and ^{13}C NMR spectra (Table I). The infrared spectra of these unusual species resemble those of the corresponding unbridged complexes, showing strong carbonyl bands in the 1650-cm^{-1} region. NMR studies confirmed the structure of the products, and the assignments are illustrated in Figure 1. The monomeric nature of the complexes was established by electron bombardment mass spectrometry, which showed the expected molecular peak. Molecular weight was confirmed in one case by direct determination with vapor pressure osmometry (Table III).

Electrochemical Studies. The results of cyclic voltammetric studies on the model and lacunar complexes are given in Table IV (measured in 0.1 M TBAT/CH_3CN vs Ag/0.1 M $AgNO_3$/CH_3CN reference electrode). Each complex shows a reversible wave in the range 0.65–0.75 V, followed by an irreversible oxidation at 1.1–1.4 V. By analogy with the much studied nickel(II) cyclidene complexes,[43-47] these processes can be assigned to the $Ni^{III/II}$ couple and a ligand oxidation, respectively.

From the data in Table IV, it is clear that bridging has no effect on the $Ni^{III/II}$ redox potential since, for a given parent Schiff base, $E_{1/2}$ is the same within experimental error for the model and the bridged complexes. This result is reminiscent of the insensitivity of $E_{1/2}$ to bridge length noted for the lacunar cyclidene complexes[43-47] and is probably due to the absence of strong axial ligation to nickel in *either* the Ni^{II} or Ni^{III} species.[46,47] Further, this suggests that the formation of the bridge does not distort the interactions of the substituent.

The potentials are, however, influenced by the nature of the substituents on the chelate backbone. The complexes with R^3 = Me gave $E_{1/2}$ values roughly 110 mV lower than those measured for the analogous complexes with R^3 = H. The cathodic shift in redox potential is consistent with the electron-donating nature of the methyl groups relative to hydrogen. In addition to the obvious inductive effect mentioned above, there may be an additional resonance effect as a result of bond rotations in the unsaturated portions of the ligand imposed by the bulky methyl groups.[48]

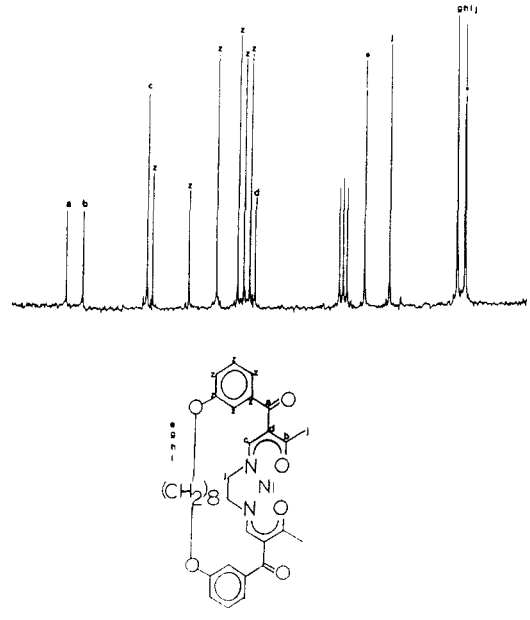

Figure 1. $^{13}C\{^1H\}$ NMR spectrum for $Ni(Me_2R^2H_2malen)$ measured in $CDCl_3$; $SiMe_4$ standard.

The electrochemical reversibility of the first electrode process for the model and bridged complexes is itself noteworthy, given the total irreversibility of the electrochemistry of the parent complexes.[48] Further, the voltammograms of the monoacylated complexes (structure X) are also totally irreversible, with anodic

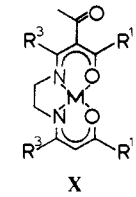

X

peak potentials falling between those of the parent and the diacylated complexes. The reversibility of the redox process bodes well for the probability of resistance of the derived oxygen carriers toward autoxidation by mechanisms that produce irreversible higher valent species or that subsequently produce ligand oxidation. This distinctive electrochemical behavior also provides a convenient technique for monitoring the progress of the bridging reactions and assessing product purity.

Crystal Structures. Structure determinations have been completed on the two lacunar complexes having $R^1 = R^3 = CH_3$ (compound A) and $R^1 = CH_3$ and $R^3 = H$ (compound B). The first of these, compound A, the "tetramethyl" complex, presents

(43) Busch, D. H.; Olszanski, D. J.; Stevens, J. C.; Schammel, W. P.; Kojima, M.; Herron, N.; Zimmer, L. L.; Holter, K. A.; Mocak, J. *J. Am. Chem. Soc.* **1981**, *103*, 1472.

(44) Busch, D. H.; Jackels, S. C.; Callahan, R. W.; Grzybowski, J. J.; Zimmer, L. L.; Kojima, M.; Olszanski, D. J.; Schammel, W. P.; Stevens, J. C.; Holter, K. A.; Mocak, J. *Inorg. Chem.* **1981**, *20*, 2834.

(45) Korybut-Daszkiewicz, B.; Kojima, M.; Cameron, J. H.; Herron, N.; Chavan, M. Y.; Jircitano, A. J.; Coltrain, B. K.; Neer, G. L.; Alcock, N. W.; Busch, D. H. *Inorg. Chem.* **1984**, *23*, 903.

(46) Chavan, M. Y.; Meade, T. J.; Busch, D. H.; Kuwana, T. *Inorg. Chem.* **1986**, *25*, 314.

(47) Chavan, M. Y. Ph.D. Thesis, The Ohio State University, 1983.

(48) Goldsby, K. A.; Jircitano, A. J.; Minahan, D. M.; Ramprasad, D.; Busch, D. H. *Inorg. Chem.* **1987**, *26*, 2651.

Table III. Analytical Data for the New Complexes

complex	R^1	R^3	formula	calcd % C	calcd % H	calcd % N	calcd % Cl	found % C	found % H	found % N	found % Cl
VIII	CH_3	CH_3	$C_{34}H_{40}NiN_2O_6 \cdot 2CHCl_3$	49.67	4.82	3.21	24.49	49.82	5.07	3.26	24.67
VIII[a]	CH_3	H	$C_{32}H_{36}N_2NiO_6 \cdot {}^3/_4CH_2Cl_2$	58.97	5.62	6.20	7.98	58.58	5.59	4.05	8.23
IX	CH_3	CH_3	$C_{28}H_{30}N_2NiO_6$	61.23	5.46	5.10		60.77	5.82	5.00	
IX	CH_3	H	$C_{26}H_{26}N_2NiO_6$	59.92	4.99	5.38		59.45	5.21	5.33	

[a] Molecular weight by vapor pressure osmometry: calcd, 666.46; found, 659.

Table IV. Cyclic Voltammetry Data[a] for the New Nickel(II) Complexes in Acetonitrile

structure	R^1	R^3	$E_{1/2,1}$, V	ΔE_{p1},[b] V	E_{p2},[c] V
IX	Me	H	0.74	0.07	1.43
IX	Me	Me	0.63	0.08	1.30
VIII	Me	H	0.74	0.09	1.5[d]
VIII	Me	Me	0.64	0.07	1.31

[a] Potentials measured at a platinum disk working electrode in 0.1 M TBAT/CH_3CN vs a Ag/0.1 M $AgNO_3/CH_3CN$ reference electrode; scan rate is 100 mV/s. [b] ΔE_p is the interval between the anodic and cathodic peak potentials. [c] This value is the peak potential for the second, irreversible oxidation process. [d] Broad.

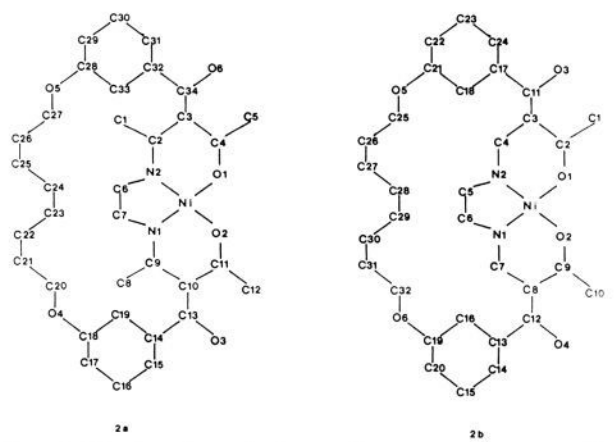

Figure 2. Number schemes for the crystal structures: (a) compound A [Ni($Me_2R^2Me_2$malen)]; (b) compound B [Ni($Me_2R^2H_2$malen)].

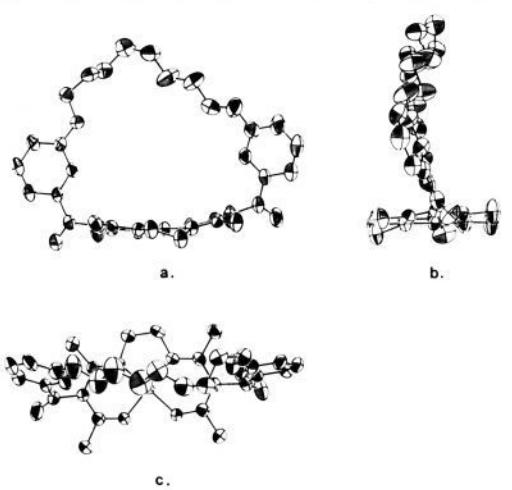

Figure 3. ORTEP diagrams for lacunar Schiff base compound A [Ni($Me_2R^2Me_2$malen)].

a rather ideal stereochemistry and a remarkable example of inclusion chemistry and will be discussed first. The "dimethyl, dihydrogen" compound shows the structural flexibility that results from insufficient steric bulk in the parent Schiff base ligand, a subject that will be discussed as a major consideration in ligand design.

Structure of Compound A ($R^1 = CH_3$, $R^3 = CH_3$). The atomic numbering scheme is given in Figure 2a, and ORTEP drawings are presented in Figure 3. Tables V and VI contain selected bond lengths and bond angles while Table VII contains atomic coordinates.

The ORTEP drawings (Figure 3a–c) show that the lacunar structure is very nearly ideal with the bridge soaring above the coordination plane where it is suspended by the aromatic risers. The aromatic rings are almost perpendicular to the plane of the

Table V. Bond Lengths for [Ni($Me_2R^2Me_2$malen)]·$2CHCl_3$

bond	length, Å	bond	length, Å
N1–Ni	1.843 (5)	C14–C13	1.482 (9)
N2–Ni	1.848 (5)	O3–C13	1.209 (7)
O1–Ni	1.854 (4)	C15–C14	1.395 (9)
O2–Ni	1.841 (4)	C19–C14	1.373 (9)
C7–N1	1.467 (7)	C16–C15	1.374 (10)
C9–N1	1.302 (7)	C17–C16	1.360 (11)
C2–N2	1.317 (8)	C18–C17	1.369 (10)
C6–N2	1.467 (8)	C19–C18	1.389 (9)
C4–O1	1.288 (7)	O4–C18	1.367 (9)
C11–O2	1.290 (7)	C20–O4	1.385 (10)
C2–C1	1.513 (8)	C27–O5	1.433 (7)
C3–C2	1.426 (8)	C28–O5	1.349 (7)
C4–C3	1.371 (8)	C29–C28	1.381 (8)
C34–C3	1.503 (8)	C33–C28	1.384 (8)
C5–C4	1.497 (9)	C30–C29	1.362 (9)
C7–C6	1.492 (8)	C31–C30	1.379 (9)
C9–C8	1.514 (8)	C32–C31	1.395 (8)
C10–C9	1.416 (8)	C33–C32	1.382 (8)
C11–C10	1.382 (8)	C34–C32	1.482 (9)
C13–C10	1.502 (8)	O(6)–C34	1.213 (7)
C12–C11	1.505 (8)		

Table VI. Bond Angles for [Ni($Me_2R^2Me_2$malen)]·$2CHCl_3$

bonds	angle, deg	bonds	angle, deg
N2–Ni–N1	87.9 (2)	C10–C11–O2	124.3 (6)
O1–Ni–N1	177.4 (2)	C12–C11–O2	114.0 (6)
O1–Ni–N2	94.1 (2)	C12–C11–C10	121.7 (6)
O2–Ni–N1	93.2 (2)	C14–C13–C10	117.6 (6)
O2–Ni–N2	177.6 (2)	O3–C13–C10	122.4 (6)
O2–Ni–O1	84.9 (2)	O3–C13–C14	119.9 (6)
C7–N1–Ni	110.6 (4)	C15–C14–C13	119.4 (7)
C9–N1–Ni	128.0 (4)	C19–C14–C13	120.6 (6)
C9–N1–C7	121.3 (5)	C19–C14–C15	120.0 (7)
C2–N2–Ni	127.3 (4)	C16–C15–C14	119.1 (8)
C6–N2–Ni	112.6 (4)	C17–C16–C15	121.6 (8)
C6–N2–C2	119.4 (5)	C18–C17–C16	119.1 (8)
C4–O1–Ni	126.8 (4)	C19–C18–C17	121.1 (8)
C11–O2–Ni	127.0 (4)	O4–C18–C17	114.5 (8)
C1–C2–N2	118.8 (6)	O4–C18–C19	124.4 (7)
C3–C2–N2	121.9 (5)	C18–C19–C14	119.1 (7)
C3–C2–C1	119.3 (6)	C20–O4–C18	119.0 (7)
C4–C3–C2	123.5 (6)	C28–O5–C27	118.3 (5)
C34–C3–C2	119.2 (6)	C29–C28–O5	125.5 (7)
C34–C3–C4	117.3 (6)	C33–C28–O5	115.3 (6)
C3–C4–O1	125.2 (6)	C33–C28–C29	119.1 (6)
C5–C4–O1	113.4 (6)	C30–C29–C28	120.1 (7)
C5–C4–C3	121.3 (6)	C31–C30–C29	121.1 (7)
C7–C6–N2	109.1 (5)	C32–C31–C30	119.6 (7)
C6–C7–N1	108.1 (5)	C33–C32–C31	118.6 (6)
C8–C9–N1	119.2 (6)	C34–C32–C31	119.0 (6)
C10–C9–N1	121.9 (6)	C34–C32–C33	122.4 (6)
C10–C9–C8	118.6 (5)	C32–C33–C28	121.3 (6)
C11–C10–C9	122.9 (5)	C32–C34–C3	119.2 (6)
C13–C10–C9	118.7 (6)	O6–C34–C3	120.4 (6)
C13–C10–C11	118.3 (6)	O6–C34–C32	120.4 (6)

Table VII. Non-Hydrogen Atomic Coordinates for $[Ni(Me_2R^2Me_2malen)]\cdot 2CHCl_3$

atom	x	y	z
Ni	0.42271 (6)	0.46568 (3)	0.21552 (3)
N1	0.2677 (4)	0.5086 (2)	0.2228 (2)
N2	0.4331 (4)	0.5191 (2)	0.1398 (2)
O1	0.5756 (3)	0.4185 (2)	0.2094 (2)
O2	0.4182 (3)	0.4145 (2)	0.2924 (2)
O3	0.1211 (4)	0.4374 (2)	0.4179 (2)
O4	0.3621 (5)	0.7271 (2)	0.4411 (2)
O5	0.8668 (3)	0.7165 (2)	0.1945 (2)
O6	0.7809 (4)	0.4473 (2)	0.0417 (2)
C1	0.5262 (5)	0.5812 (3)	0.0508 (2)
C2	0.5325 (5)	0.5268 (3)	0.1064 (2)
C3	0.6437 (5)	0.4838 (3)	0.1199 (2)
C4	0.6567 (5)	0.4317 (3)	0.1679 (2)
C5	0.7721 (5)	0.2846 (3)	0.1770 (3)
C6	0.3212 (5)	0.5648 (3)	0.1237 (2)
C7	0.2146 (5)	0.5370 (3)	0.1592 (2)
C8	0.0773 (5)	0.5498 (3)	0.2691 (3)
C9	0.2044 (5)	0.5117 (3)	0.2741 (2)
C10	0.2456 (4)	0.4753 (3)	0.3332 (2
C11	0.3443 (5)	0.4259 (3)	0.3379 (2)
C12	0.3735 (5)	0.3793 (3)	0.3981 (3)
C13	0.1736 (5)	0.4867 (3)	0.3921 (2)
C14	0.1719 (5)	0.5610 (3)	0.4200 (2)
C15	0.0705 (6	0.5822 (3)	0.4543 (3)
C16	0.0709 (7)	0.6507 (4)	0.4812 (3)
C17	0.1682 (7)	0.6977 (4)	0.4757 (3)
C18	0.2687 (6)	0.6761 (3)	0.4431 (3)
C19	0.2711 (6)	0.6078 (3)	0.4143 (2)
C20	0.4810 (7)	0.7051 (4)	0.4262 (4)
C21	0.5608 (8)	0.7743 (4)	0.4215 (4)
C22	0.6863 (7)	0.7621 (4)	0.4045 (4)
C23	0.7623 (7)	0.8301 (4)	0.3959 (3)
C24	0.8989 (9)	0.8147 (4)	0.3874 (3)
C25	0.9270 (6)	0.7751 (3)	0.3255 (3)
C26	0.8955 (6)	0.8186 (3)	0.2637 (3)
C27	0.9383 (6)	0.7824 (3)	0.2040 (3)
C28	0.8901 (5)	0.6729 (3)	0.1442 (3)
C29	0.9789 (5)	0.6857 (3)	0.1004 (3)
C30	0.9940 (5)	0.6373 (3)	0.0514 (3)
C31	0.9188 (5)	0.5762 (3)	0.0431 (2)
C32	0.8287 (5)	0.5621 (3)	0.0869 (2
C33	0.8161 (5)	0.6108 (3)	0.1371 (2)
C34	0.7529 (5)	0.4944 (3)	0.0791 (2)
C91	0.5882 (6)	0.2366 (3)	0.7865 (3)
C92	0.6842 (6)	0.4929 (3)	0.3511 (3)
Cl1	0.4420 (2)	0.2792 (1)	0.7941 (1)
Cl2	0.6818 (2)	0.2922 (1)	0.7410 (1)
Cl3	0.3330 (2)	0.7236 (1)	0.6357 (1)
Cl4	0.8315 (2)	0.4517 (1)	0.3609 (1)
Cl5	0.6359 (3)	0.5096 (2)	0.4285 (1)
Cl6	0.6864 (4)	0.5703 (1)	0.3068 (1)

chelate, and this orientation can be attributed to the presence of the bulky methyl groups at both the R^1 and R^3 positions as revealed by the deviation from this ideal geometry that occurs in the structure of compound B (see below). This vertical orientation of risers also causes the polymethylene chain to span directly across the chelate plane. The angle between the planes defined by C32, C34, O6 and C2, C3, C4 is 69.2°, and the angle between the planes C9, C10, C11 and C14, C13, O3 is 60.6°. The elevated polymethylene chain creates a spacious void in the complex. The void width, which is defined as the distance between C19 and C33, the closest two carbon atoms in each of the two aromatic rings, is 8.47 Å. The void height, which is the average distance from Ni to C23 and C24, the two middle atoms in the polymethylene chain, is about 8.51 Å. These dimensions are sufficiently large for the void to accept a bent O_2 molecule without significant repulsion.

A particularly fascinating and unexpected example of inclusion chemistry results from the cavity of this compound and is shown in Figure 4. The presence of the lacuna and the packing of the molecules facilitate the accommodation of two chloroform molecules, one on each side of the pocket, as solvent of crystallization.

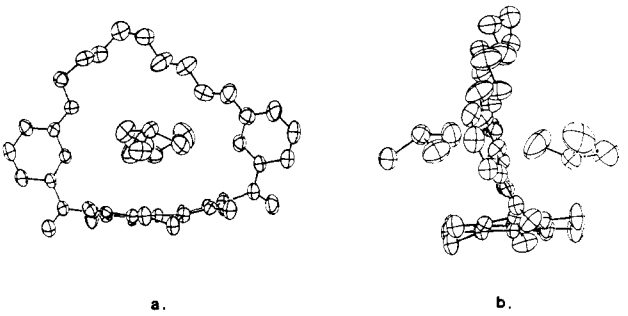

Figure 4. ORTEP diagrams showing the orientation of the $CHCl_3$ molecules with respect to the cavity in compound A $[Ni(Me_2R^2Me_2malen)]$.

Table VIII. Bond Lengths for $[Ni(Me_2R^2H_2malen)]\cdot 2CH_2Cl_2$

bond	length, Å	bond	length, Å
O1–Ni	1.865 (7)	C17–C11	1.459 (14)
O2–Ni	1.837 (8)	O4–C12	1.223 (15)
N1–Ni	1.802 (8)	C13–C12	1.538 (18)
N2–Ni	1.816 (8)	C14–C13	1.389 (16)
C2–O1	1.295 (12)	C16–C13	1.372 (17)
C9–O2	1.277 (12)	C15–C14	1.400 (18)
C6–N1	1.411 (11)	C20–C15	1.327 (18)
C7–N1	1.266 (11)	C19–C16	1.387 (20)
C4–N2	1.308 (10)	C18–C17	1.352 (13)
C5–N2	1.483 (11)	C24–C17	1.418 (14)
C2–C1	1.506 (13)	C21–C18	1.377 (16)
C3–C2	1.370 (14)	C20–C19	1.339 (20)
C4–C3	1.386 (12)	O6–C19	1.356 (18)
C11–C3	1.452 (14)	C22–C21	1.362 (17)
C6–C5	1.384 (12)	O5–C21	1.396 (16)
C8–C7	1.448 (14)	C23–C22	1.331 (16)
C9–C8	1.415 (14)	C24–C23	1.344 (16)
C12–C8	1.430 (16)	C25–O5	1.280 (15)
C10–C9	1.492 (13)	C26–C26	1.442 (17)
C11–O3	1.253 (12)		

Table IX. Bond Angles for $[Ni(Me_2R^2H_2malen)]\cdot 2CH_2Cl_2$

bonds	angle, deg	bonds	angle, deg
O2–Ni–O1	87.0 (3)	C10–C9–C8	123.8 (12)
N1–Ni–O1	178.3 (4)	O3–C11–C3	121.7 (13)
N1–Ni–O2	93.9 (4)	C17–C11–C3	120.6 (11)
N2–Ni–O1	93.3 (4)	C17–C11–O3	117.5 (12)
N2–Ni–O2	177.2 (4)	O4–C12–C8	126.7 (16)
N2–Ni–N1	86.0 (4)	C13–C12–C8	117.5 (14)
C2–O1–Ni	127.6 (7)	C13–C12–O4	115.7 (15)
C9–O2–Ni	130.3 (8)	C14–C13–C12	117.7 (18)
C6–N1–Ni	113.7 (7)	C16–C13–C12	123.5 (17)
C7–N1–Ni	126.2 (8)	C16–C13–C14	118.8 (16)
C7–N1–C6	119.6 (10)	C15–C14–C13	116.8 (16)
C4–N2–Ni	126.3 (7)	C20–C15–C14	125.2 (19)
C5–N2–Ni	112.5 (7)	C19–C16–C13	119.5 (16)
C5–N2–C4	121.1 (9)	C18–C17–C11	122.3 (13)
C1–C2–O1	110.8 (11)	C24–C17–C11	119.8 (13)
C3–C2–O1	125.1 (11)	C24–C17–C18	117.8 (13)
C3–C2–C1	124.1 (11)	C21–C18–C17	117.7 (13)
C4–C3–C2	120.3 (11)	C20–C19–C16	122.9 (19)
C11–C3–C2	121.2 (11)	O6–C19–C16	123.8 (21)
C11–C3C4	118.4 (11)	O6–C19–C20	112.3 (24)
C3–C4–N2	127.2 (11)	C19–C20–C15	116.2 (21)
C6–C5–N2	109.7 (10)	C22–C21–C18	124.3 (15)
C5–C6–N1	110.7 (10)	O5–C21–C18	124.0 (15)
C8–C7–N1	127.9 (12)	O5–C21–C22	111.6 (18)
C9–C8–C7	118.2 (11)	C23–C22–C21	117.5 (17)
C12–C8–C7	120.4 (12)	C24–C23–C22	121.0 (16)
C12–C8–C9	121.1 (13)	C23–C24–C17	121.6 (14)
C8–C9–O2	122.6 (12)	C25–O5–C21	118.8 (16)
C10–C9–O2	113.5 (12)	C26–C25–O5	113.4 (18)

The carbon atom in one of the two chloroforms is 3.32 and 3.29 Å from the two oxygen atoms in the coordination sphere. The hydrogen atom is directed toward the midpoint between the two oxygen atoms, with atom–atom separations corresponding to hydrogen-bonding distances.

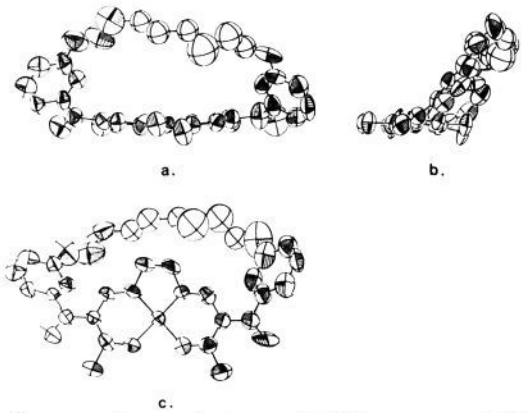

Figure 5. ORTEP diagrams for lacunar Schiff base compound B [Ni-($Me_2R^2H_2$malen)].

Table X. Non-Hydrogen Atomic Coordinates of [Ni($Me_2R^2H_2$malen)]·$2CH_2Cl_2$[a]

atom	x	y	z
Ni	0.6260 (1)	0.4878 (1)	−0.0057 (1)
N1	0.6431 (6)	0.4926 (5)	0.1200 (6)
N2	0.6844 (6)	0.5817 (5)	−0.0056 (6)
O1	0.6057 (5)	0.4853 (4)	−0.1358 (4)
O2	0.5731 (5)	0.3907 (4)	−0.0058 (5)
O3	0.6754 (7)	0.6576 (5)	−0.3228 (6)
O4	0.5368 (12)	0.2481 (7)	0.2247 (7)
O5	1.0680 (10)	0.6888 (8)	−0.1069 (9)
O6	0.8978 (12)	0.3751 (8)	0.4269 (11)
C1	0.6068 (8)	0.5100 (7)	−0.2942 (7)
C2	0.6352 (9)	0.5350 (8)	−0.1953 (8)
C3	0.6859 (8)	0.6014 (7)	−0.1724 (8)
C4	0.7060 (8)	0.6213 (6)	−0.0794 (7)
C5	0.7111 (10)	0.6104 (7)	0.0903 (7)
C6	0.6622 (11)	0.5671 (7)	0.1546 (8)
C7	0.6294 (8)	0.4386 (7)	0.1766 (8)
C8	0.5968 (9)	0.3612 (7)	0.1551 (9)
C9	0.5647 (9)	0.3436 (7)	0.0615 (10)
C10	0.5204 (9)	0.2685 (6)	0.0310 (8)
C11	0.7216 (10)	0.6515 (7)	−0.2441 (8)
C12	0.5876 (14)	0.3066 (8)	0.2284 (11)
C13	0.6493 (15)	0.3209 (7)	0.3215 (11)
C14	0.6009 (12)	0.3100 (7)	0.4038 (13)
C15	0.6585 (18)	0.3230 (9)	0.4878 (11)
C16	0.7499 (16)	0.3411 (8)	0.3271 (13)
C17	0.8170 (11)	0.6931 (7)	−0.2286 (8)
C18	0.8935 (11)	0.6675 (7)	−0.1695 (8)
C19	0.7978 (15)	0.3578 (9)	0.4138 (18)
C20	0.7551 (16)	0.3444 (9)	0.4946 (12)
C21	0.9825 (14)	0.7087 (10)	−0.1639 (10)
C22	0.9992 (12)	0.7724 (10)	−0.2155 (11)
C23	0.9234 (15)	0.7972 (9)	−0.2733 (12)
C24	0.8340 (11)	0.7604 (8)	−0.2806 (8)
C25	1.0598 (13)	0.6366 (9)	−0.0451 (15)
C26	1.1394 (14)	0.6387 (11)	0.0285 (14)
C27	1.1176 (17)	0.5877 (11)	0.1113 (15)
C28	1.0818 (17)	0.5885 (12)	0.1822 (16)
C29	1.0690 (14)	0.5356 (12)	0.2636 (13)
C30	0.9839 (21)	0.5173 (18)	0.2904 (20)
C31	1.0199 (19)	0.4669 (15)	0.3713 (19)
C32	0.9443 (17)	0.4123 (13)	0.3701 (14)
Cl1	0.7686 (4)	0.6504 (3)	0.3907 (4)
Cl2	0.6489 (12)	0.5288 (8)	0.4452 (6)
Cl22	0.5984 (14)	0.5605 (9)	0.4404 (7)
C99	0.6868 (16)	0.6185 (12)	0.4727 (13)

[a] Occupancy factor for Cl_2 is 0.56 (3) and for Cl_{22} is 0.44 (3). Occupancy factor for all other atoms is 1.0.

Structure of Compound B ($R^1 = CH_3$, $R^3 = H$). The atom-numbering scheme is given in Figure 2b, and an ORTEP plot is shown in Figure 5. Tables VIII and IX contain selected bond lengths and bond angles while Table X contains atomic coordinates. Unlike the ideal structure presented above, in this case the polymethylene chain spans across the plane of the metal chelate at an angle that tilts the bridge down toward the malen plane. The angle between the planes defined by O3, C11, C17 and C2, C3, C4 is 33.2°, and the angle between the planes defined by O4, C12, C13 and C7, C8, C9 is 19.4°. Thus, the structure is intermediate between the ideal one for lacuna formation and a contrasting structure in which the strap lies approximately coplanar with the coordination plane. The conjugation around atoms C3 and C11 and also C8 and C13 should favor this hypothetical *flat* structure, and this may be a factor contributing to the small angle between the strap and the coordination plane. On the other hand, the interaction between the pairs of hydrogen atoms attached to C4 and C18 and those on C7 and C16 militates against formation of the totally planar structure. The contrast between the structures of compounds A and B emphasizes the need for suitable molecular design to assure that risers lift the bridge above the coordination plane in attempts to produce molecular cavities in structures of this kind. The probability that this interpretation is correct is enhanced by the recent study on the closely related diacetyl tetramethyl- and dimethylmalen complexes. Crystal structures show that the acetyl groups are coplanar with the chelate rings in the case of the dimethylmalen complex while they are more nearly perpendicular to the chelate rings in the tetramethylmalen derivatives.[48]

Table XI. Summary of Crystal Structure Data

	compound A	compound B
formula	$NiC_{34}H_{40}N_2O_6 \cdot 2CHCl_3$	$NiC_{32}H_{36}N_2O_6 \cdot 2CH_2Cl_2$
MW	870.2	688.3
a, Å	10.608 (2)	13.205 (3)
b, Å	18.388 (4)	17.497 (3)
c, Å	20.492 (4)	14.315 (5)
α, deg	90.00	90.00
β, deg	95.35 (2)	93.59 (2)
γ, deg	90.00	90.00
V, Å^3	3980 (2)	3301 (2)
Z	4	4
space gp	$P2_1/c$	$P2_1/n$
ρ_{calcd}	1.45	1.39
ρ_{measd}	1.45	1.43
radiat	Mo Kα (λ = 0.71069 Å)	Mo Kα (λ = 0.71069 Å)
scan type	θ–2θ	ω–2θ
2θ range, deg	4–50	4–55
no. of unique reflcns	6216	4608
no. of reflcns with $F_o^2 > 3\sigma(F_o^2)$	4078	3496
cryst dimens, mm	0.31 × 0.33 × 0.37	0.50 × 0.40 × 0.45
μ, cm^{-1}	8.79	7.50
no. of param	460	358
R^a	0.051	0.106
R_w^b	0.050	0.092
diffractometer	Syntex, P$\bar{1}$	Enraf-Nonius CAD4

[a] $R = \sum||F_o| - |F_c||/|F_o|$. [b] $R_w = [\sum w(||F_o| - |F_c||)^2/\sum w|F_o|^2]^{1/2}$.

The packing diagram reveals that pairs of molecules of the complex are packed very close together in a back-to-back fashion. The distance between the Ni in one complex and that in the second complex is 3.37 Å. This distance is just 0.2–0.3 Å longer than the Ni–Ni distance in some macrocycle complexes, which are considered to be dimers.[49–51] The positioning of the solvent in this structure is unremarkable.

Experimental Section

X-ray Structure Determination. Table XI summarizes the crystal structure data.

Data Collection. Both of the data sets were collected by a similar method on red crystals that were stable at room temperature. Background counts were taken with a background to scan ratio of 0.5 at the beginning and end of each 2θ scans. The data were corrected for background, and Lorentz and polarization factors were applied to obtain structure factors. No absorption correction was applied. $\sigma(F_o^2)$ was obtained with counting statistics.

(49) Stephens, F. S.; Vagg, R. S. *Inorg. Chim. Acta* **1980**, *42*, 139.
(50) Charlson, A. J.; Stephens, F. S.; Vagg, R. S.; Watton, E. C. *Inorg. Chim. Acta* **1977**, *25*, L51.
(51) Stephens, F. S.; Vagg, R. S. *Acta Crystallogr., Sect. B: Struct. Crystallogr. Cryst. Chem.* **1977**, *B33*, 3165.

Solution and Refinement. In both of the structure determinations, the position of the heavy atom was ascertained from a Patterson map, and the positions of the remaining non-hydrogen atoms were revealed by subsequent difference Fourier maps. Refinement was performed by full-matrix least-squares techniques.[52] Computer programs used were SHELX and ORTEP.[53]

For complex A ($R^1 = CH_3$, $R^3 = CH_3$), isotropic refinement resulted in convergence at $R = 0.123$. After anisotropic refinement of all non-hydrogen atoms and refinement including hydrogen atoms in fixed position, the final least-squares cycle resulted in convergence at $R = 0.051$ and $R_w = 0.050$ with $w = 1/\sigma^2(F_o)$. The value of the highest peak in the final difference Fourier map was 0.6 e/Å^3. No disorder was observed.

For complex B ($R^1 = CH_3$, $R^3 = H$), isotropic refinement resulted in convergence at $R = 0.144$. Full anisotropic refinement led to extremely large and nonpositive-definite thermal parameters for the carbon atoms C27, C28, C29, C30, C31, and C32 of the polymethylene bridge. This must result from disorder in the bridge, but we were unable to model this with partial atoms; it was necessary to use isotropic temperature factors for these atoms. Hydrogen atoms were placed in calculated positions and included in the structure calculations but were not refined. A disorder of the CH_2Cl_2 molecules was also encountered, and multipositions for Cl atoms were used. Final least-squares refinement resulted in convergence at $R = 0.106$ and $R_w = 0.092$ with $w = 1/\sigma^2(F_o)$. In the final difference Fourier map, only one peak had a value of over 1.0 e/Å^3, and this was in the vicinity of the CH_2Cl_2 molecules. The relatively poor final R value is clearly attributable to the disorder in part of the structure and the difficulty of modeling this satisfactorily. However, apart from the geometry of the chain, the structure of the complex is satisfactorily defined.

Materials. Solvents and reagents were dried rigorously before using. Benzene, triethylamine, and acetonitrile (for electrochemical measurements) were dried by refluxing over CaH_2, followed by distillation under nitrogen. Electrochemical grade tetra-*n*-butylammonium tetrafluoroborate (TBAT) was purchased from Southwestern Analytical Co. and used as received. The precursor complexes, structure VI, were prepared by published procedures.[54,55]

Physical Measurements. ^{13}C NMR spectra were recorded on a Bruker WP80 (20.115-MHz) spectrometer. Infrared spectra were obtained on KBr pellets with a Perkin-Elmer Model 457 spectrophotometer. Elemental analyses and osmometric molecular weight determinations were performed by Galbraith, Inc., Knoxville, TN.

Electrochemical measurements were obtained on a Princeton Applied Research Model 173 potentiostat equipped with a Model 175 linear programmer. Current vs potential curves were measured on a Houston Instruments Model 2000 XY recorder. Measurements were carried out at a platinum disk in 0.1 M TBAT/CH_3CN, with a platinum wire serving as the auxiliary electrode. The potentials were measured vs a Ag/0.1 M $AgNO_3/CH_3CN$ reference electrode, which was isolated from the working and auxiliary electrodes by a fritted glass disk. Half-wave potentials were determined as the average of the peak cathodic and peak anodic potentials; i.e., $E_{1/2} = (E_{P,A} + E_{P,C})/2$. All measurements were performed in a glovebox under an atmosphere of dry nitrogen.

Syntheses. Bridging Reagent, R^2, Structure VII. A total of 6.66 g (0.289 mol) of sodium was dissolved in 350 mL of ethanol. To this was added 20 g (0.145 mol) of *m*-hydroxybenzoic acid, and the mixture was stirred until all of the acid had dissolved. 1,8-Dibromooctane (19.69 g, 0.072 mol) was added, and the reaction was held at reflux overnight. A white precipitate was observed, and this was filtered. The solid was dissolved in water, and concentrated hydrochloric acid was added until the solution was acidic. The C_8 dicarboxylic acid precipitated from solution and was isolated by filtration. It was redissolved in concentrated potassium hydroxide solution and then reprecipitated by the addition of concentrated hydrochloric acid. This final precipitate was filtered, washed, and dried in vacuo for several days until the solid was crusty. This crusty, white solid was recrystallized from hot dioxane, producing a 23% yield (6.5 g, 0.017 mol) of the C_8 dicarboxylic acid.

The acid was refluxed with an excess of thionyl chloride. After 2 h, all of the solid was observed to dissolve to give a yellow solution. The thionyl chloride was removed by distillation, leaving a dark yellow oil. Benzene was added, and the solution was rotary evaporated to dryness. The latter procedure was repeated a second time. The contents of the flask were extracted with hot hexane which, on cooling, gave the C_8 diacid chloride in 61% yield (4.4 g, 0.01 mol): Ir C=O at 1770 cm^{-1}; NMR, see Table I.

Lacunar Nickel Complex, Compound A. [**Ni(Me$_2$R^{2}Me$_2$malen)**]. A total of 1.7 g (6.05 mmol) of the precursor nickel complex (structure VI, $R^1 = R^3 = CH_3$) and 2.7 g (6.4 mmol) of the C_8 diacid chloride, prepared as described above, were dissolved in 2 L of dry benzene containing 3 g of triethylamine. The mixture was kept under reflux for 10 days and then filtered to remove triethylamine hydrochloride. The solvent was removed on a rotary evaporator, and the resulting solid was chromatographed on an alumina column. An orange-red band was eluted with chloroform, and it yielded a red crystalline solid upon addition of hexane, yield 2.3 g (3.7 mmol, 60%).

Lacunar Nickel Complex, Compound B [**Ni(Me$_2$R^{2}H$_2$malen)**]. A total of 0.9 g (3.56 mmol) of the precursor nickel complex (structure VI, $R^1 = CH_3$, $R^3 = H$) and 1.53 g (3.63 mmol) of the C_8 acid chloride, prepared as described above, were dissolved in 1500 mL of dry benzene containing 1.5 mL of triethylamine. The solution was refluxed for 6 days, with 1 mL of triethylamine being added after 2 days of reflux. The triethylamine hydrochloride was filtered, and the solvent was removed by rotary evaporation. The orange-red oil was dissolved in a minimum amount of chloroform and chromatographed on alumina column. The fast-moving orange-red band was collected upon elution with chloroform. An orange-red solid was obtained by the addition of ethanol and reduction of the volume of the mixed solvent. This solid was recrystallized from methylene chloride and petroleum ether to give about 0.6 g (1 mmol), 28% of the lacunar nickel complex.

Model Compound [**Ni(Me$_2$(*m*-Anyl)$_2$Me$_2$malen)**]. The precursor complex (1.90 g, 6.77 mmol, structure VI, $R^1 = R^3 = CH_3$) was dissolved in 200 mL of dry benzene, and 1.37 g (13.5 mmol) of triethylamine was added, followed by 2.30 g (13.5 mmol) of *m*-anisoyl chloride. The mixture was maintained at reflux for 3 days with stirring. The triethylamine hydrochloride was filtered, and the solvent was removed by rotary evaporation. The contents of the flask were dissolved in a minimum volume of chloroform and chromatographed on an alumina column. A fast-moving orange-red band was collected by eluting with chloroform. The addition of ethanol, followed by reduction in the volume of the mixed solvent, resulted in the precipitation of the desired complex, yield, 2.80 g (5.10 mmol, 75%).

Model Compound [**Ni(Me$_2$(*m*-Anyl)$_2$H$_2$malen)**]. The precursor complex (0.73 g, 2.89 mmol, structure VI, $R^1 = CH_3$, $R^3 = H$) was dissolved in 125 mL of dry benzene, and 0.82 mL of triethylamine was added, followed by 0.82 mL of *m*-anisoyl chloride. After reflux for 60 h, the solution was worked up as described for the other model complex. Yield of orange-red product was approximately 1 g (2 mmol, 65%).

Acknowledgment. The partial support of the National Science Foundation and of Air Products and Chemicals, Inc. is gratefully acknowledged.

Supplementary Material Available: Tables of thermal parameters and hydrogen atom coordinates and figures of packing diagrams (10 pages); listings of observed and calculated structure factors (46 pages). Ordering information is given on any current masthead page.

(52) Scattering factors and anomalous dispersion factors were taken from: *International Tables for X-ray Crystallography*; Kynoch: Birmingham, England, 1974; Vol. IV.

(53) (a) Sheldrick, G. M. SHELX76, *Computing in Crystallography*; University of Cambridge: Cambridge, England, 1978. (b) ORTEP, Report ORNL-5138, 3rd rev.; Oak Ridge National Laboratory: Oak Ridge, TN.

(54) Wolf, L.; Jager, E. *Z. Anorg. Allg. Chem.* **1966**, *346*, 76.

(55) McCarthy, P. J.; Hovey, R. J.; Ueno, K.; Martell, A. E. *J. Am. Chem. Soc.* **1955**, *77*, 5820.